Quasi-periodic Sphere Packing Generated by Random Ballistic Deposition Model in Confined Space

Lin Hao, Ming Yuan, Qi Liu, Bingwen Hu and Chengjie Xia*

Shanghai Key Laboratory of Magnetic Resonance, Institute of Condensed Matter Physics and Materials, School of Physics and Electronic Science, East China Normal University, Shanghai 200241, P. R. China

Abstract: Packing structures in confined space are typically different from those on a two-dimensional plane or in an infinitely-large volume. One fundamental question about packing problem is the influence of space dimension on packing structures, especially for two- and three-dimensional packing which are directly related to many condensed matter and soft material systems, while packing in confined space may serve as a connection in between. Here, we study packing of spheres generated by random ballistic deposition model in a container whose width is slightly larger than sphere diameter. The packing structure in such quasi-two-dimensional space inherits characteristics of both two- and three-dimensional packing, such as long correlation length and geometric frustration. Scaling relationships between correlation length, a structural order parameter and the container width have been established. It is demonstrated that this model system has a geometric phase transition and the rigorous two-dimensional system is a critical point. The intrinsic metastability and ergodicity-breaking of random deposition have also been discussed, which resembles the glass transition phenomenon.

Packing problems are optimization problems of arranging a large number of objects in a container [1], and they are also directly related to various condensed-matter and soft materials [2-4]. To satisfy different optimization targets and constraints, objects with different shapes may be packed into either regular or irregular patterns [5-7], and they may also depend on the packing-generating protocols. In general, the typical packing structure is strongly influenced by the dimensions and sizes of the container. Most packing problems relevant to materials in the physical world are in two- or three-dimensional (2D or 3D) space, and the characteristic packing structures generally depend on the space dimension. For example, for identical hard spheres (or disks) in 2D, a regular hexagonal pattern is the closest packing structure both locally and globally, while the closest local structure in 3D is a tetrahedral cluster, which fails to tile space and is incompatible with the densest periodic face-centered-cubic packing [1]. In spherical colloidal or granular systems, which are experimental models of hard spheres [8,9], geometric frustration (see Ref. [10]) leads to metastable random packing states and glassy dynamics with spontaneous ergodicity breaking, and their phase behaviors are fundamentally different from the 2D hard sphere melting transition [11]. Obviously, the distinct dynamic and thermodynamic phenomena of particulate systems originate from their packing structures strongly affected by the different dimensions in space. Therefore, it is fundamental to study how dimension of the space embedding the packing affects its structure.

On the other hand, if the width of a 3D container along one direction is not much larger than the objects, the packing inside may exhibit even more extraordinary structures [12-18], and such confined space is considered to be quasi-2D, which has an effective space dimension between two and three [18]. For example, the structure of colloidal monolayer between two parallel walls separated by a small gap displays an approximate hexagonal symmetry and a novel geometric frustration [15]. Therefore, it seems that quasi-2D packing inherits structural attributes of both 2D and 3D systems, and hence, it

establishes a unique connection between them. By altering the confinement width to change gradually the effective space dimension, we can study its influence on packing structures in a continuous fashion.

In the present work, quasi-2D packing of identical spheres are generated following a random ballistic deposition (RBD) model [19-25], and the packing is confined between two parallel walls with a small separation gap slightly larger than sphere diameter (Fig. 1(a)). The major finding is that the periodicity previously observed in 2D RBD packing (see Ref. [23,24]) is partly preserved with additional randomness in this quasi-2D system. We refer such packing structures as being quasi-periodic since they are in between being strictly periodic and amorphous (as in a 3D RBD packing [20,21]). Both persistent length and uniformity of the quasi-periodic structures show scaling relationships with the gap width of the container. Hence, a rigorous 2D system can be regarded as a geometric singular point. In the following, we first describe the model, and then briefly revisit some elementary characteristics of the 2D packing structure before we systematically analyze the quasi-2D system.

In RBD model, each sphere is deposited sequentially into a container and rolls down previously-established spheres following the steepest descent path under gravity, until it stops at a first stable position supported by sidewalls and (or) other spheres and remains there permanently (Fig. 1(b)). It is clear that all complex dynamics during packing formation such as particle collision and bouncing are neglected in this model, which can be realized through a sedimentation experiment of frictional granular spheres in highly viscous liquid. The RBD and other similar stochastic models of hard sphere systems are important tools to study non-equilibrium packing-formation of different condensed-matter phases and soft materials [19,20,26,27]. For example, RBD model has been used to comprehend crucial geometric attributes of the complex dynamics and heterogeneous phases of granular materials [25,28-30].

Previous studies have demonstrated an unexpected spontaneous development of periodic structures of RBD packing in 2D (see Ref. [23,24]). To generate packing in rigorous 2D space, identical spheres are dropped into a container with a rectangular cross-section with short side length (gap width) w_s being equal with the sphere diameter, and the length of its long side is w_l. All length scales in this work are expressed in unit of sphere diameter. The *x*- (*y*-) axis of the coordinate system is defined along the short (long) side of the container (Fig. 1(b)), and the origin of coordinate is set at the center of the cross-section. In 2D RBD packing, the smallest packing segment that repeats itself along the vertical direction is defined as a unit cell (Fig. 1(c)). The structures of unit cells in different realizations of RBD packing are stochastic as spheres are dropped from random initial positions, but they always satisfy the following topological law. Each unit cell is composed of n zig-zag chains of $n+1$ spheres which contact with others sequentially along the chain, with the first and last spheres in touch with the container wall at $y=\pm w_l/2$ (Fig. 1(c)). Therefore, the size of each unit cell, that is the number of spheres within, is always equal to some "magic number": $n(n+1)$. We refer the integer n as a topological index of each cell. Periodic patterns can thus be categorized according to n. A simple geometric argument leads to the conclusion that n essentially satisfies: $2(w_l-1)/\sqrt{3} \le n \le 2(w_l-1)$, due to the fact that the angles between the horizontal plane and most bonds between contacting spheres are in the range $[\pi/6, \pi/3]$ (see Ref. [31]).

If w_s is slightly larger than one, and each sphere is dropped from above at a random position with its *x*- and *y*-coordinate sampled randomly from uniform distributions between $\pm(w_s-1)/2$ and $\pm(w_l-1)/2$ respectively, a quasi-2D RBD packing structure can be generated. In this work, we analyzed RBD packing for different w_s ranging from 1 to 1.5, and fix the value of w_l at 5. For each w_s value, we generate 600 different packing structures and each packing contains $N_{tot}=10^5$ spheres. We have verified that all following major conclusions remain unchanged for $w_l=4$. In quasi-2D

packing with all w_s values covered in this study, above topological law for 2D system remains the same (Fig. 1(c)). Therefore, "unit cells" in quasi-2D RBD packing can be recognized by simply counting the topological index n. However, the structures of different "unit cells" along the vertical direction are slightly distorted compared with each other, and such pattern is therefore quasi-periodic.

We first quantify the distortion of "unit cells" in quasi-2D RBD packing. An average relative displacement of spheres in two "unit cells" is defined as the minimum value of:

$$\Delta(l)=\sqrt{\frac{1}{n(n+1)}\sum_{i=1}^{n(n+1)}\left|\boldsymbol{r}_i+l\boldsymbol{e}_z-\tilde{\boldsymbol{r}}_i\right|^2}\,, \tag{1}$$

as a function of l, where $\boldsymbol{r}_i$ and $\tilde{\boldsymbol{r}}_i$ are the coordinates of the *i*th pair among the $2n(n+1)$ spheres in two adjacent "unit cells", and $\boldsymbol{e}_z$ is the unit vector of the *z*-axis (along the vertical direction). Its minimum value $\Delta_{min}=\Delta(l^*)$ corresponds to a best match of the two "unit cells" when the structure of one cell is moved vertically, and l^* represents a "lattice-constant" (Fig. 2(a)). Δ_{min} equals zero for periodic patterns in a 2D RBD packing, while in quasi-2D space, Δ_{min} is positive and fluctuates around its average $\langle\Delta_{min}\rangle$. Occasionally, Δ_{min} of one batch of $n(n+1)$ spheres is much larger than $\langle\Delta_{min}\rangle$, which corresponds to the ends of quasi-periodic patterns. As shown in Fig. 1(d-f), one quasi-periodic pattern may terminate spontaneously, and after a short transient non-periodic pattern, it evolves into another quasi-periodic pattern with a dissimilar "unit cell" structure. In practice, we define that one quasi-periodic pattern ends where Δ_{yz} is more than three-times larger than $\langle\Delta_{yz}\rangle$. ($\Delta_{yz}$ is defined in Eq.2, which is very similar to Δ_{min} but only relative displacements of *y* and *z*-coordinates are included.) In the following, for packing with $w_s\le 1.1$, we analyze the two major features of the quasi-periodicity in quasi-2D RBD packing: fluctuations of "unit cells" and finite pattern persistent length. For larger w_s, since it becomes difficult to tell apart "quasi-periodic" patterns from non-periodic ones, we quantify the remaining quasi-periodicity with a structural correlation function.

The average relative displacement of spheres in "unit cells", that is the structural fluctuation of "unit cells", is contributed by the three orthogonal components of $\boldsymbol{\varepsilon}_i = \boldsymbol{r}_i + l^* \boldsymbol{e}_z - \boldsymbol{r}_i$, denoted as $\varepsilon_{\alpha,i}$ with $\alpha \in \{x, y, z\}$. The probability distribution function (PDFs) of $\varepsilon_{\alpha,i}$ are shown in Fig. 2(b-d). The values of ε_x is either 0 or $\pm(w_s - 1)$ with probabilities around 0.5 and 0.25 respectively. ε_x in quasi-periodic patterns with smaller n has a slightly larger probability than 0.5 to be zero. Therefore, the corresponding spheres in successive "unit cells" touch with the front or back wall at $x = \pm w_s/2$ according to a Bernoulli process with approximately equal probabilities. The PDFs of ε_y has multi-peaks, and the number of peaks depends on n and w_l in a complex way, which is beyond the scope of the present paper. The probability distribution of ε_z is close to a normal distribution with slightly boarder shoulders. Since the contribution to Δ_{min} from fluctuations of *x*-coordinate is a trivial Bernoulli distribution, we define

$$\Delta_{yz} = \sqrt{\frac{1}{n(n+1)} \sum_{i=1}^{n(n+1)} \left({\varepsilon_{y,i}}^2 + {\varepsilon_{z,i}}^2 \right)^2}, \tag{2}$$

which quantifies the average relative displacement on *yz* plane of spheres in adjacent "unit cells". The PDFs of Δ_{yz} can be collapsed onto a master curve by scaling with its average $\langle \Delta_{yz} \rangle$ (Fig. 2(e, f)). $\langle \Delta_{yz} \rangle$ follows a power-law relationship with w_s according to $\langle \Delta_{yz} \rangle \propto (w_s - 1)^{\alpha}$, with exponent $\alpha = 1.98 \pm 0.02$ (Fig. 2(g)). This power-law relationship between the quasi-periodicity and gap width reveals how randomness is gradually introduced into the packing as the space dimension increases beyond 2.

The persistent length L_p of a quasi-periodic pattern is defined as the height difference of its highest and lowest spheres. PDFs of L_p of packing with different w_s are shown in Fig. 3. Their exponential tails indicate that the beginning and termination of one quasi-periodic pattern are Poisson processes. Each exponential tail is fitted according to $p(L_p) \propto e^{-L_p/L_0}$, where L_0 is a characteristic

persistent length of the patterns. L_0 diverges as w_s decreases according to a $L_0 \propto (w_s - 1)^{-\mu}$ with $\mu = 1.85 \pm 0.18$ (inset of Fig. 3(a)). This scaling relationship implies a critical behavior with critical point at $w_s = 1$. Consistently, as w_s approaches one, the distribution evolves into a power-law distribution $p(L_p) \propto L_p^{-2}$ with a diverging first moment (Fig. 3(b)).

For w_s larger than 1.1, the average persistent length decreases to the length of only several "unit cells", and quasi-periodic patterns are basically indistinguishable from non-periodic ones. However, the remnant quasi-periodicity still causes strong structural correlation, which can be captured with a generalized pair correlation function: the vertical correlation function (VCF). A normal pair correlation function is the radial distribution of sphere centroids, and similarly, a vertical distribution function can be defined as

$$g(z) = \frac{1}{\rho}\left\langle \delta\left(z - \left|(\boldsymbol{r}_i - \boldsymbol{r}_j)\cdot \boldsymbol{e}_z\right|\right)\right\rangle, \tag{3}$$

where the average is taken over all pairs of spheres i and j, and ρ is the number density along vertical axis, *i.e.*, average number of spheres per unit height. We further divide the packing into s parts evenly along the longer side of the container, and for each part, we calculate its vertical distribution function according to:

$$g_k(z) = \frac{1}{\rho_k}\left\langle \delta\left(z - \left|(\boldsymbol{r}_i - \boldsymbol{r}_j)\cdot \boldsymbol{e}_z\right|\right)\right\rangle_k, \tag{4}$$

where $\langle\bullet\rangle_k$ means that only spheres whose *y*-coordinates are in the range $\left[(k-1)w_l/s, kw_l/s\right]$ are averaged, and $k = 1, 2, \ldots, s$. VCF of each packing is defined to be the average $g_k(z)$ of all parts and calculated according to:

$$g_z(z) = \frac{1}{s}\sum_{k=1}^{s}\frac{1}{\delta z}\int_{z-\delta_z/2}^{z+\delta_z/2} g_k(z')\,dz'. \tag{5}$$

In Eq. 5, $g_k(z)$ are further averaged over small intervals $\left[z - \delta_z/2, z + \delta_z/2\right]$ to evaluate its value

due to the delta function in Eq. (4). Compared with the simple vertical distribution function (Eq. (3)), the current definition highlights the vertical correlations of spheres with similar horizontal coordinates. This definition is motivated by the angular-dependent radial distribution function [32]. We have justified that different values of s and δ_z have only small influences on the following results, as long as s is much larger than w_l and smaller than $w_l \Big/ \sqrt{\langle \varepsilon_y{}^2 \rangle} \sim 10^2$. In this work we use $s = 20$ and $\delta_z = 0.6$.

For each w_s, an average VCF $\langle g_k(z) \rangle$ of 600 different packing is calculated and shown in Fig. 4(a). The first peak of VCF corresponds to the correlation between two adjacent "unit cells". Their height g_{max} are basically constant for $w_s \le 1.1$ and decrease exponentially with w_s for $w_s > 1.1$ (Fig. 4(b)). The vertical correlation associated with quasi-periodicity essentially vanishes beyond a characteristic gap width around 1.3, which can be regarded as a threshold beyond which a quasi-2D experimental system should not be considered as 2D any longer. Additionally, an exponential decay of evenly-spaced peaks can be clearly observed, which is directly related to the non-uniformity of "unit cells", and the average distance between peaks is none other than the average lattice-constant l^*.

A more interesting fact about VCF is that even for a same w_s, VCFs of different packing are not essentially the same, especially when w_s is close to one. This unique feature of correlation functions of quasi-2D RBD packing demonstrates an unexpected geometric ergodicity breaking. During the stochastic deposition, as more and more spheres are added into the packing, the highest "unit cell' explores different configurations. However, since the system size (N_{tot}) is finite, the average number of different quasi-periodic patterns in one packing is also limited, which is proportional to N_{tot}/L_0 and decreases to one as w_s approaches one. In other words, the "unit cells" in one packing can explore all possible configurations compatible with the container only if N_{tot} goes to infinity. Therefore, packing with small w_s contains just a few different quasi-periodic patterns and each

individual pattern has its unique contribution to the vertical correlation, so that their VCFs differ from one another. Comparatively, packing with relatively large w_s has enough number of different independent patterns, so that their VCFs are fully-averaged and are statistically identical with each other.

Because of this ergodicity breaking, there are two different ways to define and calculate the average correlation length of VCF. The first one is an ensemble-averaged correlation length $\langle \xi \rangle$, which is the fit coefficient of the peaks of average VCFs according to: $\langle g_z \rangle \propto e^{-z/\langle \xi \rangle}$. A second configurational-averaged correlation length $\bar{\xi}$ is obtained by first fitting the peaks of each individual packing's VCF according to $g_z \propto e^{-z/\xi}$, and then averaging all coefficients ξ to obtain $\bar{\xi}$. For $w_s > 1.1$, $\langle \xi \rangle$ are basically equal to $\bar{\xi}$, and they show a scaling relationship with w_s as $\xi \propto (w_s - 1)^{-\nu_h}$ with $\nu_h = 1.7 \pm 0.3$. In contrast, the two correlation length deviates noticeably from each other for $w_s \leq 1.1$, as $\langle \xi \rangle$ basically saturate to a constant and $\bar{\xi}$ are much larger which shows a scaling relationship $\bar{\xi} \propto (w_s - 1)^{-\nu}$ with a new exponent $\nu = 0.47 \pm 0.15$ (Fig. 4(c)). The divergency of $\bar{\xi}$ with w_s clearly demonstrates that the rigorous 2D packing structure resembles a critical point of a "zero-temperature" second-order phase transition. In addition, the diverging correlation length (and persistent length of quasi-periodic structure) and the underlying ergodicity breaking remind us of the typical glassy dynamics [33]. In a glassy system, when temperature is lowered below the glass-transition temperature (as w_s gets smaller than 1.1), the system falls out of equilibrium and essentially gets stuck in one configuration, so that its time-scale of reconfiguration (which is analogous to $\bar{\xi}$ of RBD packing) increases drastically.

Finally, to further depict above critical behavior of quasi-2D RBD packing, we define an order parameter of this geometric phase transition as the average probability of spheres to have four contacts. In 2D packing prepared by RBD, most spheres have four contacts, and those with three or five contacts

can be identified as defects [34,35]. For our quasi-2D packing with different w_s, the probability distributions $p(c)$ of contact number c are shown in Fig. 5(a). With w_s decreases towards one, both $p(3)$ and $p(5)$ decrease, and $p(4)$ increases following a scaling relationship according to $1-p(4)\propto(w_s-1)^{\beta}$ with exponents $\beta=0.50\pm0.03$ for $w_s\le1.1$ (inset of Fig. 5(a)). This exponent as well as the exponent ν of diverging correlation-length are both surprisingly close to their respective mean-field values. Furthermore, the underlying ergodicity breaking of this critical behavior can also be evidenced by the fluctuations of contact number probability. The standard variances of $p(c)$ of 600 packing structures for each w_s are calculated and denoted as $\sigma_p(c)$ (Fig. 5(b)). For $w_s\le1.1$, $\sigma_p(c)$ with $c=3,4,5$ demonstrate scaling relationships with w_s-1 according to $\sigma_p(c)\propto(w_s-1)^{-\gamma}$ with $\gamma=0.52\pm0.08$. $\sigma_p(c)$ combines the fluctuations of both quasi-periodic pattern structures and numbers of independent patterns within each packing. Intuitively, as previously discussed, the number of independent patterns in one packing decreases with w_s, which naturally leads to larger fluctuation of $p(c)$. As w_s gets larger, enough randomness is introduced into the system, so that the ergodicity is restored and $\sigma_p(c)$ decreases. For $w_s>1.1$, the complex dependence of $\sigma_p(c)$ on w_s suggests competitions between different sources of fluctuations, and may imply hidden additional structural transitions.

In conclusion, we analyze the packing structures generated by RBD model in quasi-2D space. Our observations suggest that the additional degree of freedom of particles' coordinates out of a 2D plane introduces randomness and demolishes spatial correlation and periodicity in a rigorous 2D system. A novel geometric phase transition is clearly demonstrated, and it is similar to another "zero-temperature" critical phenomenon previously reported in a similar system [36]. The observed criticality and metastability suggest a different perspective to understand how space dimension affects packing structures. It is also intriguing to regard the boundary-induced ordering in various packing systems as

a vestige of this critical phenomenon [37], and the random structures in the packing bulk as a geometrically "high-temperature" phase. We believe that such criticality is universal and model-independent, but may be weakened by thermal or mechanical noises in experimental systems. The universality class of RBD systems needs to be identified, and other criticalities associated with different routes away from the critical point await further studies, such as increasing particle non-sphericity and polydispersity [36]. Moreover, the intrinsic metastability emphasizes the non-equilibrium nature of the deposition process, and the complex configurational space of RBD model may help understanding glass transition as a toy-model. Last but not least, RBD packing generated in quasi-2D space provides a practical way to generate packing with controllable quenched disorder and correlation length, which have potential application in the fabrications of functional porous media and phononic crystals.

Acknowledgements

This work is supported by the China Postdoctoral Science Foundation Grant No. 2018M641957 and No. 2019T120319, and the National Natural Science Foundation of China Grant No. 11904102.

References

[1] T. Aste and D. Weaire, *The Pursuit of Perfect Packing* (Taylor & Francis, Philadelphia, 2008).
[2] J. D. Bernal, Nature (London) **183**, 141 (1959).
[3] G. Parisi and F. Zamponi, Rev. Mod. Phys. **82**, 789 (2010).
[4] S. Torquato, J. Chem. Phys. **149**, 020901 (2018).
[5] S. Torquato and F. H. Stillinger, Rev. Mod. Phys. **82**, 2633 (2010).
[6] A. Baule, R. Mari, L. Bo, L. Portal, and H. A. Makse, Nat. Commun. **4**, 2194 (2013).
[7] S. Torquato and Y. Jiao, Phys. Rev. E **86**, 011102 (2012).
[8] C. P. Royall, S. R. Williams, T. Ohtsuka, and H. Tanaka, Nat. Mater. **7**, 556 (2008).
[9] C. Xia, J. Li, Y. Cao, B. Kou, X. Xiao, K. Fezzaa, T. Xiao, and Y. Wang, Nat. Commun. **6**, 8409, (2015).

[10] G. Tarjus, S. A. Kivelson, Z. Nussinov, and P. Viot, J. Phys. Condens. Matter **17**, R1143 (2005).

[11] A. L. Thorneywork, J. L. Abbott, D. G. A. L. Aarts, and R. P. A. Dullens, Phys. Rev. Lett. **118**, 158001 (2017).

[12] P. Pieranski, L. Strzelecki, and B. Pansu, Phys. Rev. Lett. **50**, 900 (1983).

[13] S. Neser, C. Bechinger, P. Leiderer, and T. Palberg, Phys. Rev. Lett. **79**, 2348 (1997).

[14] A. Fortini and M. Dijkstra, J. Phys. Condens. Matter **18**, L371 (2006).

[15] Y. L. Han, Y. Shokef, A. M. Alsayed, P. Yunker, T. C. Lubensky, and A. G. Yodh, Nature (London) **456**, 898 (2008).

[16] F. Ramiro-Manzano, E. Bonet, I. Rodriguez, and F. Meseguer, Soft Matter **5**, 4279 (2009).

[17] E. C. Oguz, M. Marechal, F. Ramiro-Manzano, I. Rodriguez, R. Messina, F. J. Meseguer, and H. Lowen, Phys. Rev. Lett. **109**, 218301 (2012).

[18] S. Levay, D. Fischer, R. Stannarius, B. Szabo, T. Borzsonyi, and J. Torok, Soft Matter **14**, 396 (2018).

[19] W. M. Visscher and M. Bolsterli, Nature (London) **239**, 504 (1972).

[20] C. H. Bennett, J. Appl. Phys. **43**, 2727 (1972).

[21] E. M. Tory, B. H. Church, M. K. Tam, and M. Ratner, Can. J. Chem. Eng. **51**, 484 (1973).

[22] R. Jullien and P. Meakin, Colloids Surf. A **165**, 405 (2000).

[23] P. Meakin and R. Jullien, Europhys. Lett. **15**, 851 (1991).

[24] N. Topic, T. Poschel, and J. A. C. Gallas, Phys. Rev. Lett. **120**, 148002 (2018).

[25] N. Topic, J. A. C. Gallas, and T. Poeschel, Phys. Rev. Lett. **109**, 128001 (2012).

[26] M. Rubinstein and D. R. Nelson, Phys. Rev. B **26**, 6254 (1982).

[27] D. Bideau, A. Gervois, L. Oger, and J. P. Troadec, J. Phys. (Paris) 47, 1697 (1986).

[28] J. Duran, J. Rajchenbach, and E. Clement, Phys. Rev. Lett. **70**, 2431 (1993).

[29] R. Jullien, P. Meakin, and A. Pavlovitch, Phys. Rev. Lett. **69**, 640 (1992).

[30] C. Voivret, F. Radjai, J. Y. Delenne, and M. S. El Youssoufi, Phys. Rev. E **76**, 021301 (2007).

[31] J. E. S. Socolar, Europhys. Lett. **18**, 39 (1992).

[32] C. J. Xia, Y. X. Cao, B. Q. Kou, J. D. Li, Y. J. Wang, X. H. Xiao, and K. Fezzaa, Phys. Rev. E **90**, 062201 (2014).

[33] P. G. Debenedetti and F. H. Stillinger, Nature (London) **410**, 259 (2001).

[34] N. Topic, T. Poeschel, and J. A. C. Gallas, Sci. Rep. **5**, 12703 (2015).

[35] P. Meakin and R. Jullien, Europhys. Lett. **14**, 667 (1991).

[36] F. Delyon and Y. E. Levy, J. Phys. A **23**, 4471 (1990).

[37] J. Reimann, J. Vicente, E. Brun, C. Ferrero, Y. X. Gan, and A. Rack, Powder Technol. **318**, 471 (2017).

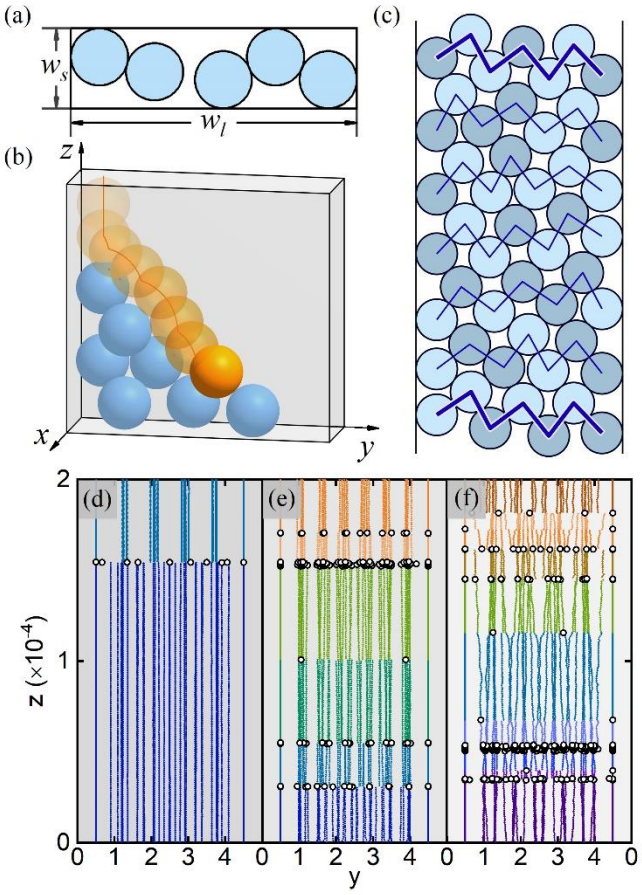

283

284 **Figure 1.** (a) A horizontal section of a quasi-2D container with short side length $w_s = 1.4$, and long
285 side length $w_l = 5$. (b) A schematic diagram of the deposition process in a quasi-2D container. A
286 sphere moves following the steepest descend path (solid curve) until it stops at the first stable position.
287 (c) "Unit cell" structures (with $n = 6$) in a quasi-2D RBD packing with $w_s = 1.04$. Centroids of
288 spheres in each zig-zag chain are connected by solid lines. The highest and lowest chain structures are
289 almost identical, which correspond to the six pairs of corresponding spheres in two adjacent "unit
290 cells". Spheres in light (dark) color are in touch with the container wall at $x = +(-)w_s/2$. (d-f)
291 Centroids of spheres in RBD packing with (d) $w_s = 1.02$, (e) 1.05 and (f) 1.1. The vertical
292 coordinates are rescaled by a factor of 10^{-4}. Centroids of spheres in same quasi-periodic patterns are
293 in same colors, and they form bunches of vertical lines which terminate at non-periodic structures.
294 Centroids of spheres in non-periodic structures are shown in circles.

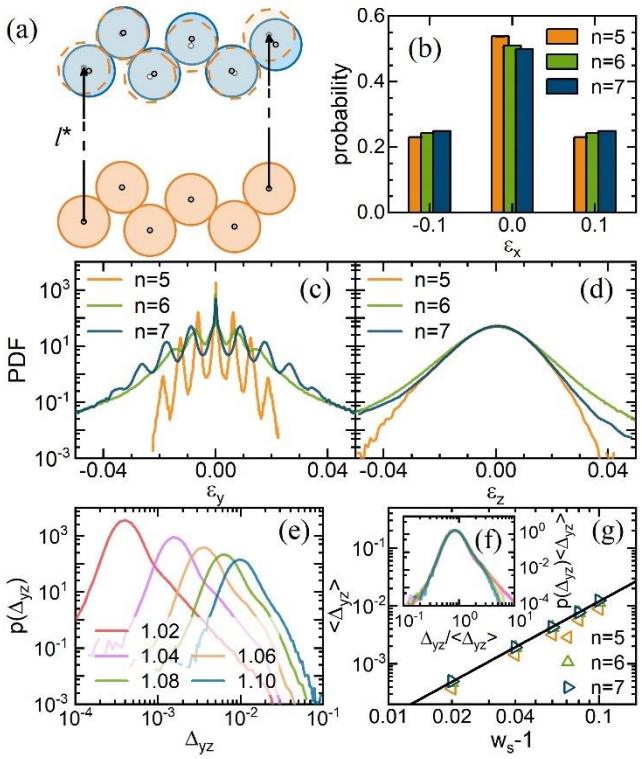

295

296 **Figure 2**. (a) A schematic diagram about the relative displacements of spheres in adjacent "unit cells".
297 All spheres in a lower "unit cell" are moved upwards by a distance l^* so that their average distance
298 to their respective corresponding spheres in the upper "cell" are minimized. (b-d) Probability
299 distributions of (b) ε_x, (c) ε_y and (d) ε_z in quasi-periodic structures with $n=5,6,7$. (e) PDF of
300 Δ_{yz} in quasi-periodic structures with $n=6$ in packing with different w_s. (f) Rescaling of $p\left(\Delta_{yz}\right)$
301 by their average values: $\left\langle \Delta_{yz} \right\rangle$. (g) $\left\langle \Delta_{yz} \right\rangle$ as a function of w_s-1 in quasi-periodic structures with
302 $n=5,6,7$. The solid line represents $\left\langle \Delta_{yz} \right\rangle \propto \left(w_s-1\right)^2$.

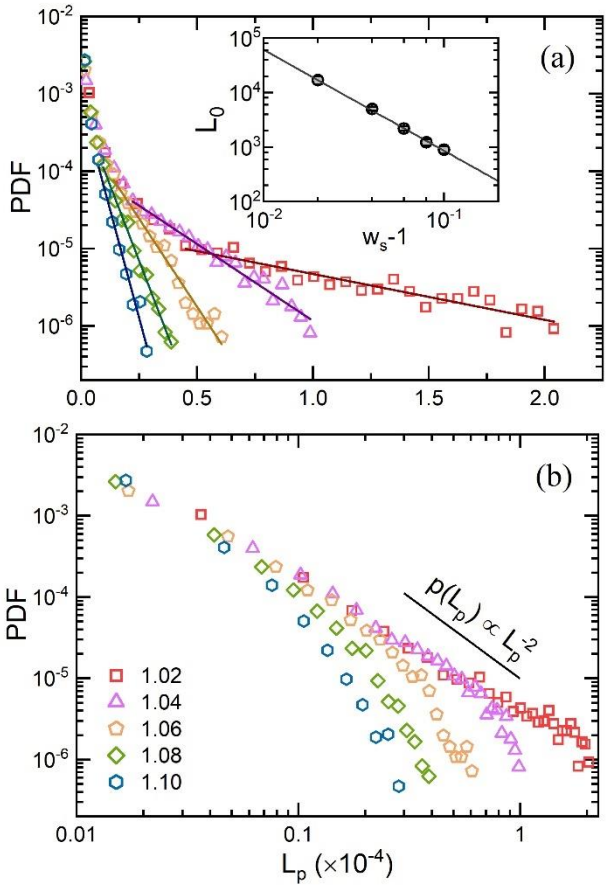

303

304 **Figure 3**. (a) Probability distribution functions of persistent length of quasi-periodic patterns in

305 packing with $w_s = 1.02$ (squares), 1.04 (triangles), 1.06 (pentagons), 1.08 (diamonds) and 1.1

306 (hexagons). The solid lines are exponential fits of the tails. (Inset) The characteristic length L_0 as a

307 function of w_s. The solid line is a power-law fit according to $L_0 \propto \left(w_s - 1\right)^{-\mu}$ with $\mu = 1.85$. (b) The

308 same distributions shown in a log-log coordinate. The solid line represents a power-law distribution

309 $p\left(L_p\right) \propto L_p^{-2}$.

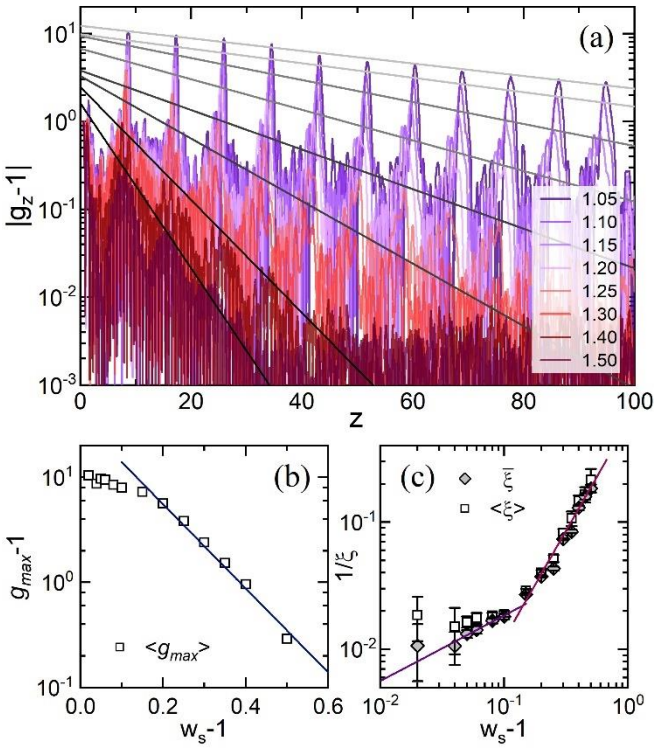

310

311 **Figure 4**. (a) Vertical correlation functions of quasi-2D RBD packing with different w_s. Each straight
312 line represents an exponential fit of the peaks. (b) The maximal peak heights of average VCFs as a
313 function of w_s. The solid line represents an exponential fit of data with $w_s > 1.1$. (c) Configurational-
314 averaged ($\bar{\xi}$) and ensemble-averaged ($\langle \xi \rangle$) correlation lengths and as a function of w_s. The two solid
315 lines represent power-law fits of the data: $\bar{\xi} \propto (w_s - 1)^{-0.47}$ for $w_s \leq 1.1$ and $\bar{\xi} = \langle \xi \rangle \propto (w_s - 1)^{-1.7}$
316 for $w_s > 1.1$ respectively.

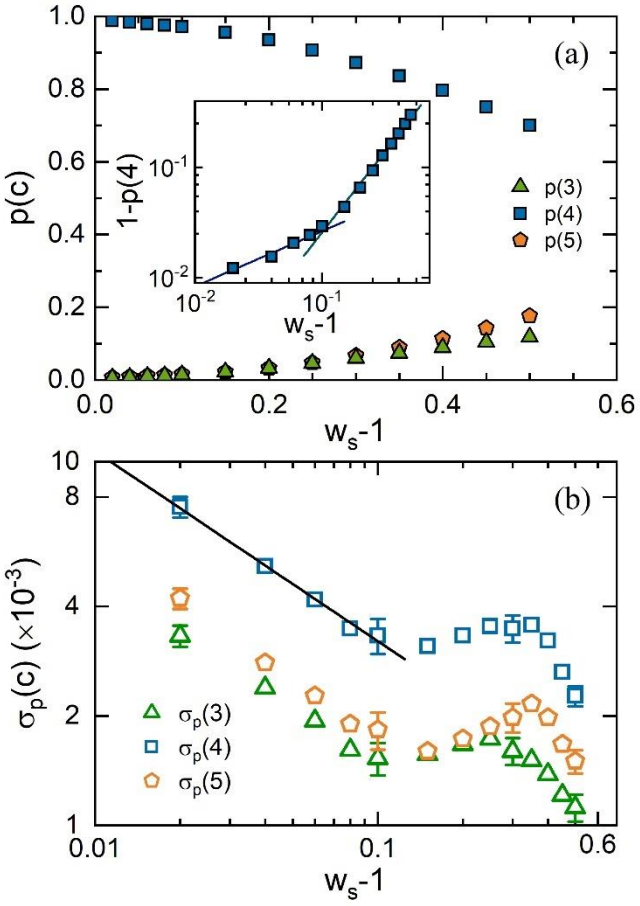

317

318 **Figure 5**. (a) Probabilities of contact numbers $c=3$ (triangles), 4 (squares) and 5 (pentagons) in

319 packing with different w_s. Spheres touching the container walls at $y=\pm w_l$ are excluded when

320 calculating the probability distributions of contact number. (Inset) $1-p(4)$ as a function of w_s-1.

321 The two solid lines represent power-law fits according to $1-p(4)\propto(w_s-1)^{\beta}$ with $\beta=0.50$ for

322 $w_s\le 1.1$ and $\beta=1.48$ for $w_s>1.1$. (b) Stand variances of $p(c)$ as a function of w_s-1. The solid

323 line represents $\sigma_p(4)\propto(w_s-1)^{-0.5}$.